Miniature Bowtie Antenna Elements and Arrays Based on Ball Grid Array Packaging for 5G Millimeter-Wave Applications

Xiubo Liu[1], Wei Zhang[1], Dongning Hao[1], and Yanyan Liu[2, *]

Abstract—This letter proposes a miniature bow-tie antenna element and its 2×2 arrays based on ball grid array (BGA) packaging technology for 5G millimeter-wave new radio (NR) applications. The antenna substrate uses ultra-economical single-layer FR4 printed circuit boards (PCB) to reduce manufacturing costs. By adopting solder balls, the antenna achieves the BGA packaging and realizes the surface mounting function. One bow-tie patch is excited by a plated through-hole (PTH) connected to the feeding point. The other bow-tie patch is directly short connected to the ground plane by another PTH. Besides, the bottom ground plane can be equivalent to a reflector, allowing the antenna element and array to obtain broadside radiation. For ease of integration, the input impedance of the antenna is set to $50\,\Omega$. The measurement results show that the $-10\,\text{dB}$ bandwidth of the antenna element is 21% covering 25.2 to 31.1 GHz. The measured peak gains of the antenna element and 2×2 arrays are 7.6 and 10.75 dBi, respectively. The proposed antenna element and array cover N257 (26.5–29.5 GHz) and N261 (27.5–28.35 GHz) bands. It is very suitable for the 5G millimeter-wave application.

1. INTRODUCTION

Due to the high path loss and rain absorption in the millimeter wave frequency band, wireless systems require tens to hundreds of antenna elements. Therefore, cost and integration are the main challenges faced by 5G millimeter-wave antennas [1, 2]. Traditional bow-tie antennas are popular because of their low cost and ease of manufacture. However, since the antenna substrate and system board are different, the coaxial line or waveguide connector will be used to interconnect with the system board [3, 4]. Nevertheless, the insertion loss between the RF front-end chip and the antenna increases simultaneously. Consequently, the performance of the RF system will degrade. On the other hand, bulky connectors are hard to integrate into the system.

Antenna-in-Package (AiP) technology provides a mainstream solution for balancing cost, size, and performance in the millimeter-wave band [5, 6]. A variety of materials can be adapted to AiP, such as low temperature cofired ceramic (LTCC) [7], glass substrate [8], stainless steel [9], and hydrocarbon ceramic organic based printed circuit board [10]. However, the cost of the above mentioned antennas is relatively high. In particular, multi-layer structures are incorporated into the antenna geometry. For large-scale applications of 5G NR, the number of antenna components used is so large that the cost cannot be ignored. FR4 is an inexpensive material that can provide a relatively cost-effective solution as an industry-standard PCB. Previous studies have successfully demonstrated that low-cost multilayer FR4 can be used for millimeter-wave frequency bands [11–13].

Inspired by the above results, a BGA packaged bowtie antenna element and its 2×2 arrays with broadband bandwidth and stable radiation beam are proposed. By adopting a single-layer FR4

substrate, the antenna element further reduces manufacturing costs. In addition, the compact three-dimensional structure allows vertical transition feed to obtain broadside radiation. Besides, the BGA packaging enables automatic assembly with other surface mount devices (SMD). Section 2 illustrates the design of the proposed antenna element. Simulated and measured results are presented in Section 3. Finally, the conclusions are given in Section 4.

2. ANTENNA DESIGN

2.1. Antenna Geometry

Figure 1 depicts the geometry of the proposed antenna element. The proposed antenna element is extremely compact and simple. It is fabricated on a single FR4 substrate with a relative permittivity of 4.4, a dielectric loss tangent of 0.02, and a thickness of 1.4 mm. It consists of two metallic bow-tie patches on the top layer, two plated through holes (PTH), one metal layer on the bottom layer, one solder resist layer, and solder balls. The metal ground plane layer can be equivalent to a reflector, enabling the antenna element to achieve broadside radiation. The annular air gap of 0.25 mm separates the RF input port from the bottom metal layer. The main bow-tie patch connects the feed point through a PTH. Another bow-tie patch is directly connected to the ground plane by another PTH. After reflow soldering, the solder balls with a diameter of 300 μm are mounted on the bottom metal layer. The solder resists layer fixes the position of the solder balls to prevent them from moving during the reflow soldering process. Vertical quasi-coaxial transmission is achieved by the solder balls. The RF input port is located on the central solder ball with an input impedance of 50 Ω, which is easy to connect with the RF chipset. Based on the antenna element, the 2×2 arrays are expanded, and the center-to-center distance between the adjacent elements is 7 mm. Finally, an antenna element of $6 \, \text{mm} \times 6 \, \text{mm} \times 1.6 \, \text{mm}$
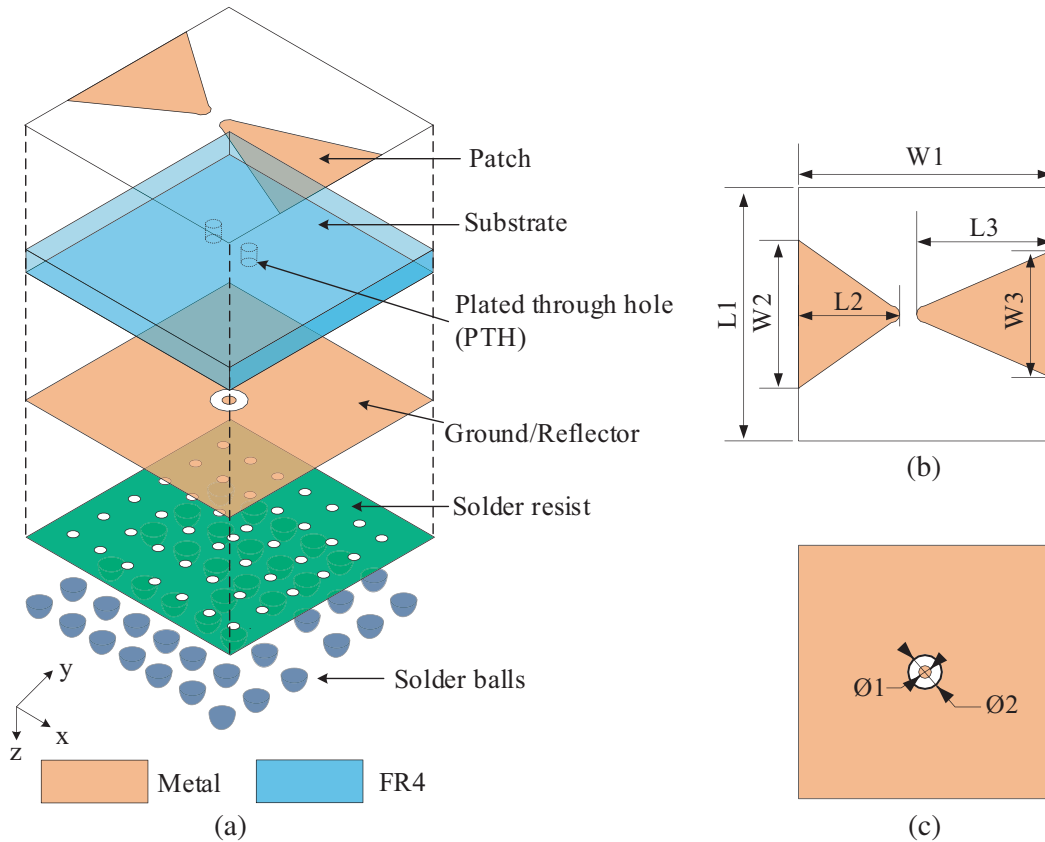

Figure 1. Geometry of the proposed antenna element. (a) Explored view. (b) Top view. (c) Bottom view.
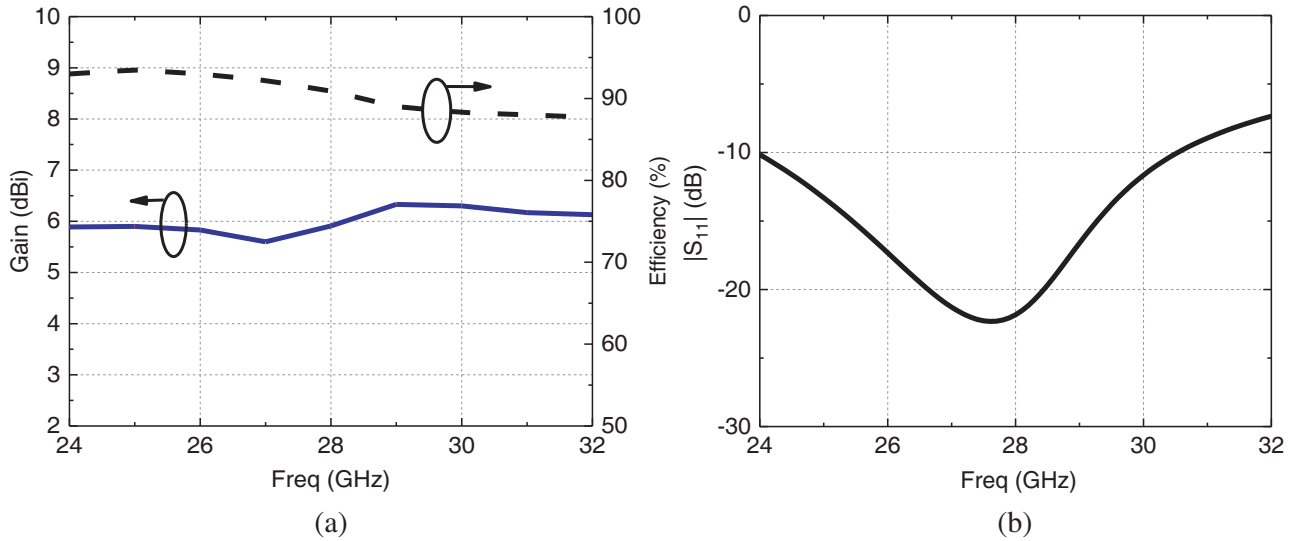
Figure 2. (a) Simulated reflection coefficient of the proposed antenna element. (b) Simulated gain and efficiency of the proposed antenna.

and a 2×2 array of $13 \, \text{mm} \times 13 \, \text{mm} \times 1.6 \, \text{mm}$ are obtained. As can be seen, the simulated reflection coefficient, gain, and efficiency of the antenna element are shown in Figures 2(a) and (b), respectively. The $-10 \, \text{dB}$ impedance bandwidth covers 24–30.5 GHz. The simulated gain is above 5.6 dBi, and the peak gain is 6.33 dBi at 29 GHz. The simulated efficiency is between 87.7% and 93.5%.

2.2. Parameter Analysis

Figure 3 shows the E-field distribution of the antenna element at 28 GHz. It can be observed that the antenna performance is mainly influenced by physical size. To better learn the influence, the parameter analysis of the key parameters ($W2$, and $W3$) is studied. In the parameter studies, only one parameter is adjusted while the other parameters remain unchanged.
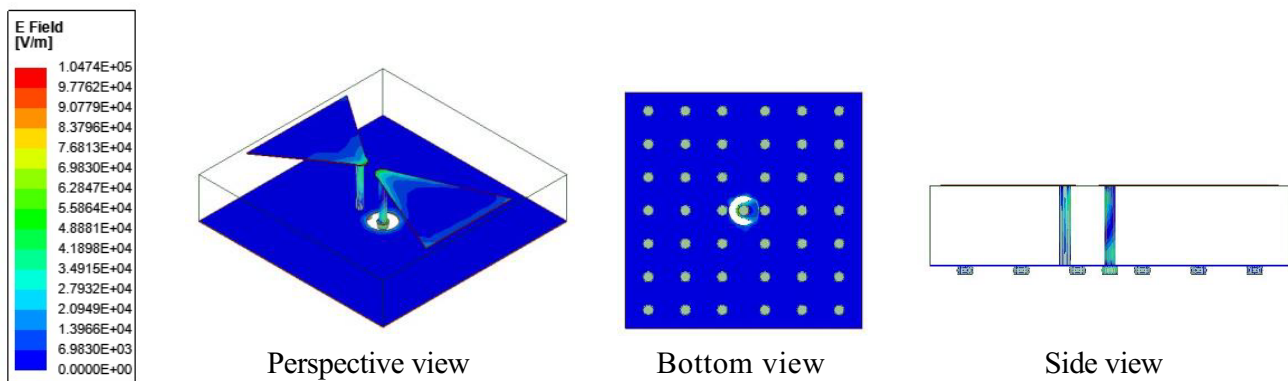

Figure 3. E-field distribution of the antenna element at 28 GHz.

As illustrated in Figure 4(a), as the width of the bow-tie patch ($W3$) increases from 0.4 to 5 mm, the 0.4 mm $W3$ has the largest impedance bandwidth of $-10 \, \text{dB}$ of 7.8 GHz, while the 5 mm $W3$ has the narrowest bandwidth of 3.6 GHz. The bandwidth decreases with the increase of $W3$. Meanwhile, as pointed out in Figure 4(b), it can be obtained that the larger the $W3$ is, the greater the antenna gain is. For instance, a $W3$ with 0.4 mm has a gain of 5.01 dBi, while a $W3$ with 5 mm has a gain of 5.64 dBi at 28 GHz. Therefore, $W3$ affects both antenna gain and impedance bandwidth simultaneously.
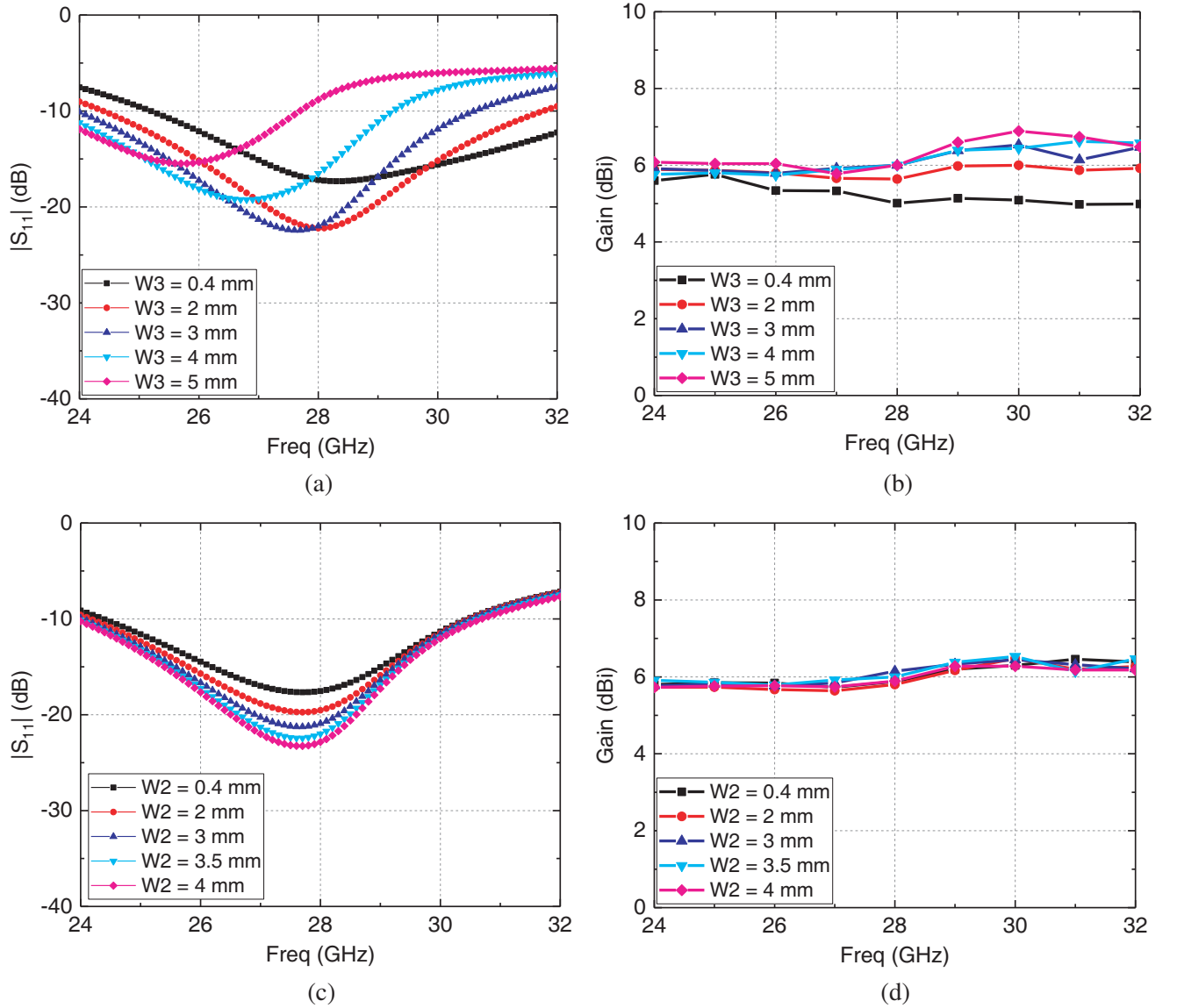
Figure 4. Simulated $|S_{11}|$ of the antenna element with different parameters. (a) $W3$. (b) $W2$. Simulated antenna gain. (c) $W3$. (d) $W2$.

To achieve better performance, after balancing the gain and impedance bandwidth of the antenna, the ultimate optimized value of $W3$ is set to 3 mm.

The parameter analysis of $W2$ is shown in Figures 4(c) and (d). It can be observed that the larger

Table 1. Dimensions of the proposed antenna element (Units: mm).

Parameters	Values	Parameters	Values
$L1$	6	$W2$	3.5
$L2$	2.4	$W3$	3
$L3$	3.2	$\Phi1$	0.3
$W1$	6	$\Phi2$	0.8

$W2$ is, the better the reflection coefficient $|S_{11}|$ is. Besides, it may also be inferred that the change of $W2$ will not be a change of the frequency band. Figure 4(d) shows the gain range of the antenna with different $W2$, and it can be observed that $W2$ has little effect on the antenna gain. Additionally, the final $W2$ is set to 3.5 mm. After performance optimization in Ansys HFSS, the detailed dimensions of the antenna element are listed in Table 1.

3. MEASUREMENT RESULTS AND DISCUSSION

As depicted in Figure 5, the prototypes of the antenna element and its 2×2 arrays are manufactured for performance verification. The proposed antenna element has a 50 Ω RF input port for interconnection with the RF chipsets. For measurement purposes, an evaluation board with a 50 Ω grounded coplanar waveguide (GCPW) line is presented to verify the performance. The evaluation board is made on a Rogers4350B with a thickness of 0.254 mm, a permittivity of 3.66, and a dielectric loss tangent of 0.004. The sizes of the evaluation board for the antenna element and 2×2 array is 23 mm $\times$ 14 mm and 34 mm $\times$ 28 mm, respectively. Three pairs of one-to-two T-junction power dividers provide four input signals with the same amplitude and phase for the 2×2 array. The 50 CPW line located on the
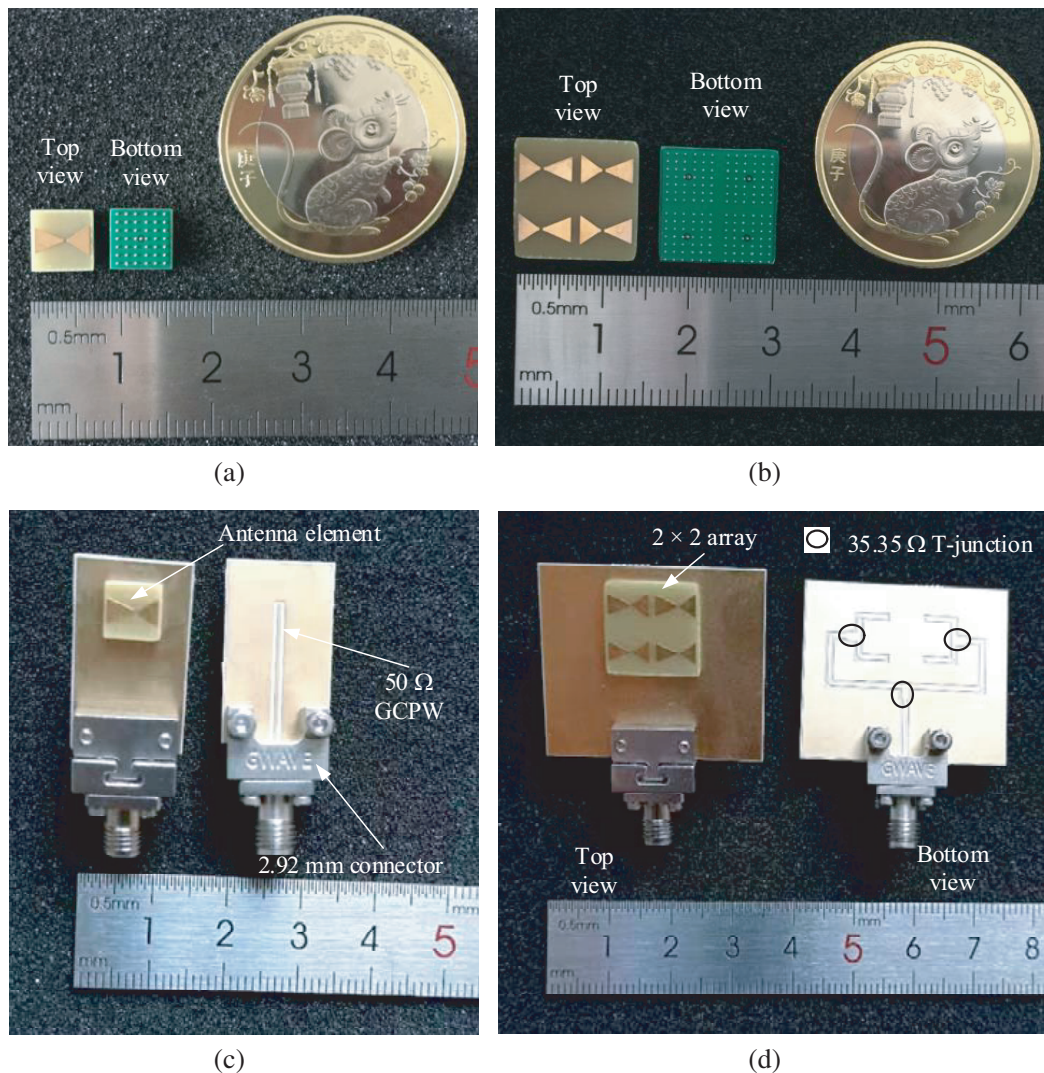

Figure 5. Photograph of the proposed antenna prototype. (a) Single element. (b) 2×2 array Assembly prototype. (c) Single element. (d) 2×2 array.

front side of the evaluation board is used to excite the backside antenna element or array. A 2.92 mm connector is mounted on the edge of the evaluation board to connect the antenna to the instrument. The S-parameters are measured by the Network Analyzer (Rohde & Schwarz, ZVA40), and the radiation characteristics are measured in a standard far-field anechoic chamber.

3.1. Experimental Results

Figure 6(a) shows the measured and simulated $|S_{11}|$ of the antenna element. The -10 dB impedance bandwidth is 21% covering 25.2 to 31.1 GHz, and the bandwidth is reduced by approximately 1 GHz compared with the simulation results. Figure 6(b) shows the measured and simulated $|S_{11}|$ of the 2×2 antenna arrays. The -10 dB impedance bandwidth ranges from 24 to 31 GHz. Figure 7(a) shows the

(a)   (b)

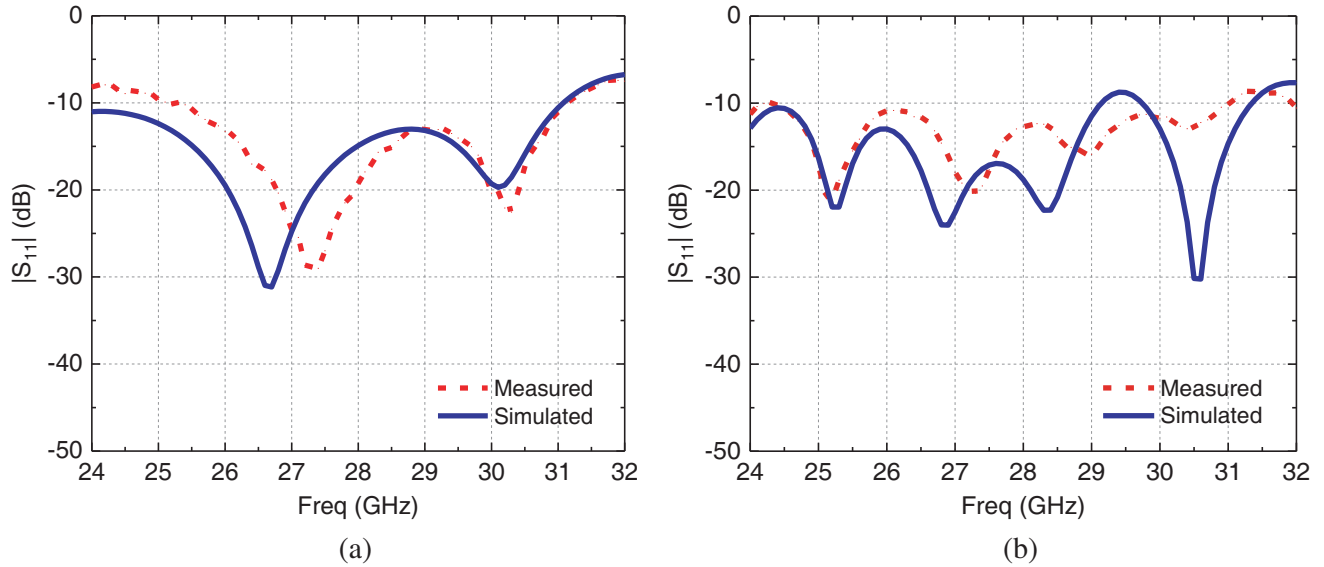**Figure 6.** Measured and simulated $|S_{11}|$ of the antenna element prototype.

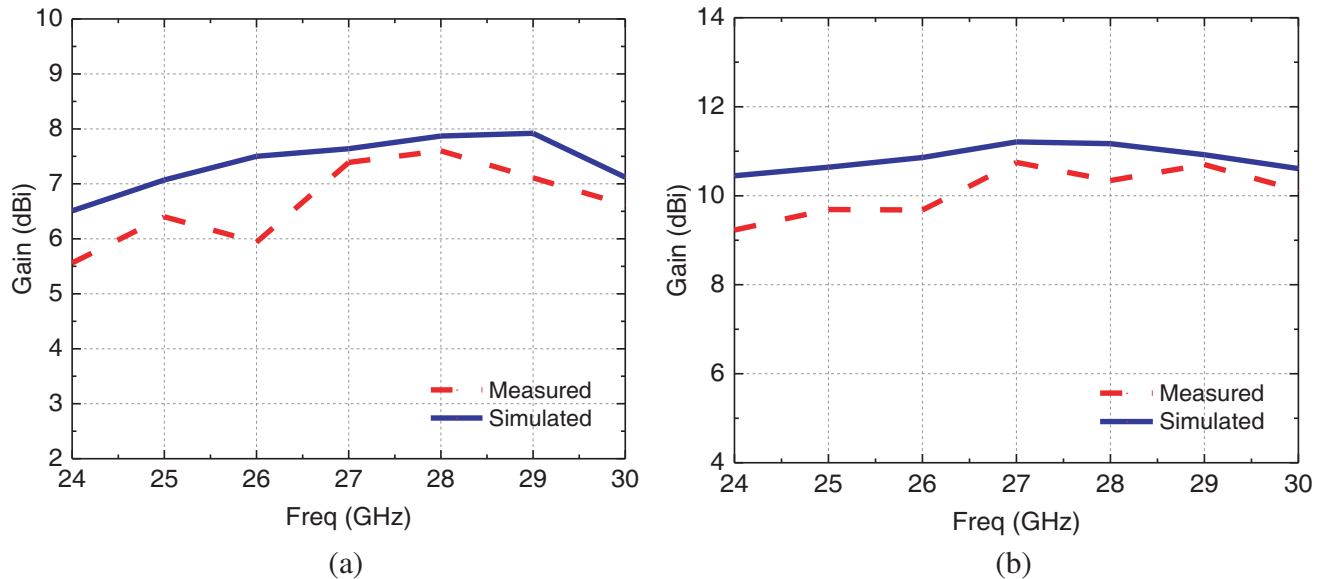(a)   (b)

Figure 7. Measured and simulated gain of the antenna element prototype.

measured and simulated maximum gains of the antenna element. The measured gain varies from 5.56 to 7.6 dBi. Figure 7(b) indicates the measured and simulated maximum gains of the 2×2 antenna array. The measured gain varies between 9.23 and 10.75 dBi. Figure 8 shows the measured and simulated radiation patterns of the proposed antenna element and 2×2 antenna array at 26, 28, and 30 GHz, respectively. In the E-plane (XOZ), the cross-polarizations level of the element is less than -13.9, -30.8, and -23 dB. The cross-polarizations level of the array is less than -17.4, -27.7, and -16 dB, respectively. In the H-plane (YOZ), the cross-polarizations level of the element is less than -18.4, -15.3, and -13.8 dB. The cross-polarizations level of the array is less than -20, -19, and -15 dB, respectively. In general, the measured results are in reasonable agreement with the simulated ones. Some discrepancies are caused by the fabrication tolerance and measurement error.
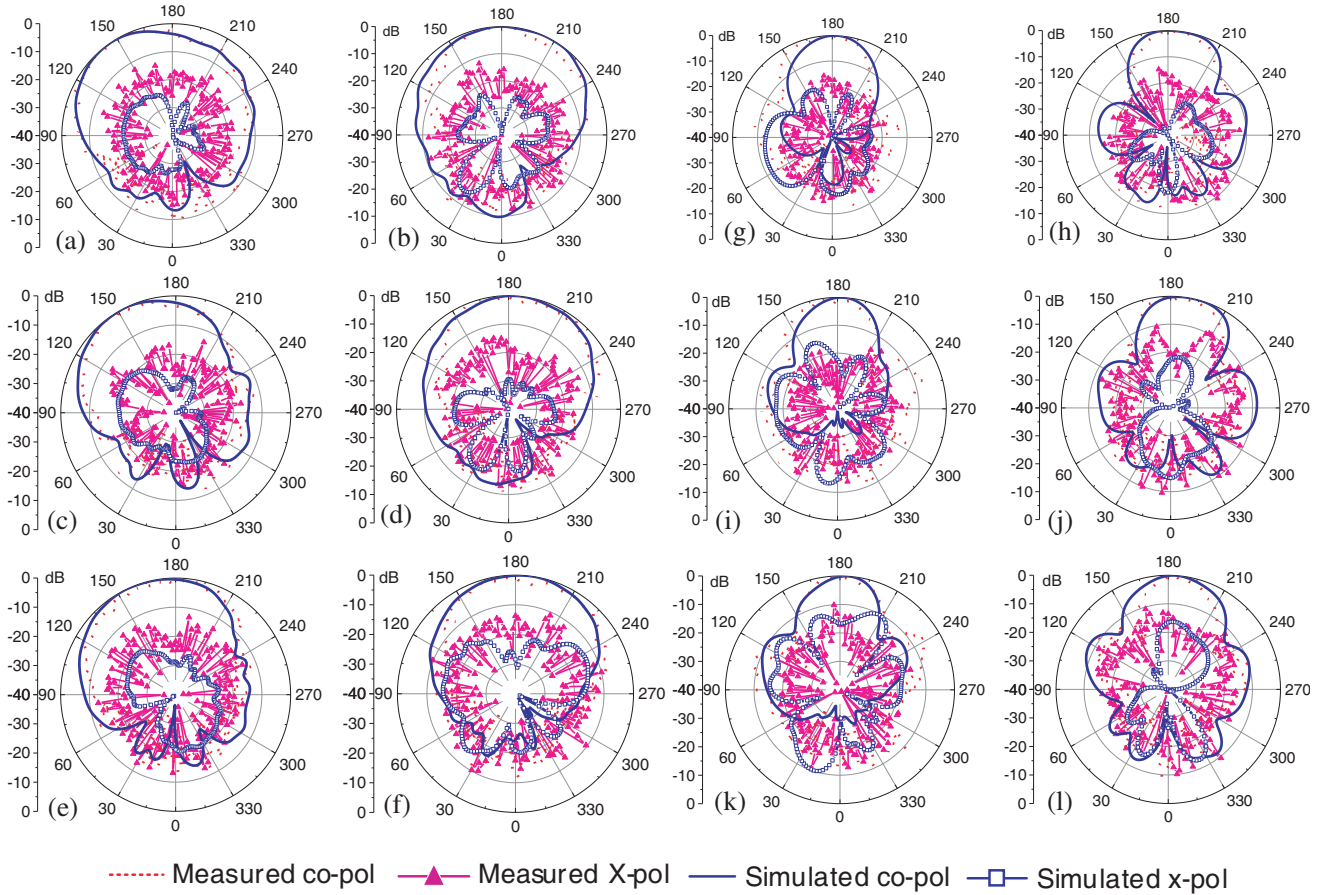

Figure 8. Measured and simulated normalization radiation patterns of the antenna element and array. (a) Element $f = 26$ GHz, E-plane. (b) Element $f = 26$ GHz, H-plane. (c) Element $f = 28$ GHz, E-plane. (d) Element $f = 28$ GHz, H-plane. (e) Element $f = 30$ GHz, E-plane. (f) Element $f = 30$ GHz, H-plane. (g) Array $f = 26$ GHz, E-plane. (h) Array $f = 26$ GHz, H-plane. (i) Array $f = 28$ GHz, E-plane. (j) Array $f = 28$ GHz, H-plane. (k) Array $f = 30$ GHz, E-plane. (l) Array $f = 30$ GHz, H-plane.

3.2. Comparison and Discussion

Table 2 summarizes the comparisons between the reported 5G NR antennas and the proposed antennas. Compared with the previous works [7–12], the proposed antenna element has higher bandwidth of 21%. In addition, a comparatively large gain of 7.1 dBi is also obtained. Benefitted from the low-cost single-layer FR4, the cost-effectiveness of the proposed antenna is also realized. The BGA package allows the antenna element to obtain a smaller size and makes it easy to integrate with other devices.

Table 2. Comparisons between the proposed and reported antenna.

Ref.	Antenna Type	F (GHz)	Imp. Bw	Max. gain (dBi)	Dimension (λ_0^3)	Material	No. of dielectric layers
[7]	PFSA	38	10.5%	2.43 (element) 7.7 (1 × 4 array)	0.69 × 0.23 × 0.11 (element) 2 × 0.23 × 0.11 (array)	LTCC	8
[8]	Yagi-Uda	26.87	19.53%	951 (1 × 4 array)	1.88 × 0.87 × 0.013	Glass	1
[9]	PIFA	28.62	2.4%	14.09 (1 × 8 array)	5.72 × 1.81 × 0.05	Stainless steel	-
[10]	Patch	30.4	2.6%	3.8 (element)	0.61 × 0.61 × −		13
[11]	PIFA	27.15	15.3%	5.85 (element)	0.4 × 0.4 × 0.12	FR4	1
[12]	Patch	33.45	15.2%	4.97 (element)	0.56 × 0.56 × 0.14	FR4	1
[13]	Patch	26.87	26.8%	7.4 (element)	0.48 × 0.48 × 0.13	FR4&RO4350B	3
This work	Bowtie	28.15	21%	7.6 (element) 10.75 (2 × 2 array)	0.57 × 0.57 × 0.15 (element) 1.2 × 1.2 × 0.15 (array)	FR4	1

4. CONCLUSIONS

In this letter, a miniature BGA packaged bow-tie antenna element and its 2 × 2 arrays have been proposed. In this design, the antenna is based on single FR4 substrate to achieve a low cost. With BGA packaging technology, the antenna can be automatically surface-mounted and integrated with other surface-mount devices. Measurement results have verified the performance of the antenna prototype. The proposed antenna element and array are suitable for the 5G NR mmWave (n257 26.5–29.5 GHz; n261 27.5–28.35 GHz) applications.

ACKNOWLEDGMENT

REFERENCES

1. Andrews, J. G., et al., "What will 5G be?" *IEEE J. Sel. Areas Commun.*, Vol. 32, No. 6, 1065–1082, Jun. 2014.

2. Roh, W., et al., "Millimeter-wave beamforming as an enabling technology for 5G cellular communications: Theoretical feasibility and prototype results," *IEEE Commun. Mag.*, Vol. 52, No. 2, 106–113, Feb. 2014.

3. Qu, S., J. Li, Q. Xue, and C. H. Chan, "Wideband cavity-backed bowtie antenna with pattern improvement," *IEEE Trans. Antennas Propag.*, Vol. 56, No. 12, 3850–3854, Dec. 2008.

4. Qu, S., K. B. Ng, and C. H. Chan, "Waveguide fed broadband millimeter wave short backfire antenna," *IEEE Trans. Antennas Propag.*, Vol. 61, No. 4, 1697–1703, Apr. 2013.

5. Zhang, Y., "Antenna-in-Package technology: Its early development [Historical corner]," *IEEE Antennas Propag. Mag.*, Vol. 61, No. 3, 111–118, Jun. 2019.

6. Zhang, Y. and J. Mao, "An overview of the development of antenna-in-package technology for highly integrated wireless devices," *Proc. IEEE*, Vol. 107, No. 11, 2265–2280, Nov. 2019.

7. Park, J., H. Seong, Y. N. Whang, and W. Hong, "Energy-efficient 5G phased arrays incorporating vertically polarized endfire planar folded slot antenna for mmWave mobile terminals," *IEEE Trans. Antennas Propag.*, Vol. 68, No. 1, 230–241, Jan. 2020.

8. Ali, M., et al., "Package-integrated, wideband power dividing networks and antenna arrays for 28-GHz 5G new radio bands," *IEEE Trans. Compon. Packag. Manuf. Technol.*, Vol. 10, No. 9, 1515–1523, Sep. 2020.

9. Park, J., D. Choi, and W. Hong, "Millimeter-wave phased-array Antenna-in-Package (AiP) using stamped metal process for enhanced heat dissipation," *IEEE Antennas Wirel. Propag. Lett.*, Vol. 18, No. 11, 2355–2359, Nov. 2019.

10. Liu, D., X. Gu, C. W. Baks, and A. Valdes-Garcia, "Antenna-in-Package design considerations for Ka-band 5G communication applications," *IEEE Trans. Antennas Propag.*, Vol. 65, No. 12, 6372–6379, Dec. 2017.

11. Wang, X., X. Liu, W. Zhang, D. Hao, and Y. Liu, "Surface-mount PIFA using ball grid array packaging for 5G mmWave," *Progress In Electromagnetics Research Letters*, Vol. 98, 55–60, 2021.

12. Wang, X., X. Liu, W. Zhang, D. Hao, and Y. Liu, "Surface mounted microstrip antenna using ball grid array packaging for mmWave systems integration," *Progress In Electromagnetics Research Letters*, Vol. 98, 105–111, 2021.

13. Lima de Paula, I., et al., "Cost-effective high-performance air-filled SIW antenna array for the global 5G 26 GHz and 28 GHz Bands," *IEEE Antennas Wirel. Propag. Lett.*, Vol. 20, No. 2, 194–198, Feb. 2021.